

## Unconventional Magnetism in a Nitrogen-Containing Analog of Cupric Oxide

A. Zorko,<sup>1,2</sup> P. Jeglič,<sup>1,2</sup> A. Potočnik,<sup>1</sup> D. Arčon,<sup>1,3</sup> A. Balčytis,<sup>4</sup> Z. Jagličić,<sup>5,6</sup> X. Liu,<sup>7</sup>  
A. L. Tchougréeff,<sup>7,8</sup> and R. Dronskowski<sup>7</sup>

<sup>1</sup>Jožef Stefan Institute, Jamova 39, 1000 Ljubljana, Slovenia

<sup>2</sup>EN-FIST Centre of Excellence, Dunajska 156, SI-1000 Ljubljana, Slovenia

<sup>3</sup>Faculty of Mathematics and Physics, University of Ljubljana, Jadranska 19, 1000 Ljubljana, Slovenia

<sup>4</sup>Institute of Applied Research, Vilnius University, Vilnius, Lithuania

<sup>5</sup>Institute of Mathematics, Physics and Mechanics, Jadranska 19, 1000 Ljubljana, Slovenia

<sup>6</sup>Faculty of Civil and Geodetic Engineering, University of Ljubljana, Jamova 2, 1000 Ljubljana, Slovenia

<sup>7</sup>Institute of Inorganic Chemistry, RWTH Aachen University, Landoltweg 1, D-52056 Aachen, Germany

<sup>8</sup>Poncelet Laboratory, Independent University of Moscow, Moscow Center for Continuous Mathematical Education, Moscow, Russia

(Received 9 May 2011; revised manuscript received 27 June 2011; published 22 July 2011)

We have investigated the magnetic properties of CuNCN, the first nitrogen-based analog of cupric oxide CuO. Our muon-spin relaxation, nuclear magnetic resonance, and electron-spin resonance studies reveal that classical magnetic ordering is absent down to the lowest temperatures. However, a large enhancement of spin correlations and an unexpected inhomogeneous magnetism have been observed below 80 K. We attribute this to a peculiar fragility of the electronic state against weak perturbations due to geometrical frustration, which selects between competing spin-liquid and more conventional frozen states.

DOI: 10.1103/PhysRevLett.107.047208

PACS numbers: 75.10.Kt, 76.30.-v, 76.60.-k, 76.75.+i

Numerous copper oxides fascinate with a plethora of exotic electronic ground states, including high-temperature superconductivity and quantum magnetism [1,2]. Many of them are low-dimensional spin-1/2 geometrically frustrated antiferromagnets (AFM) [3]. There, quantum fluctuations compete with conventional long-range ordering (LRO) and can prevail down to zero temperature, leading to cooperative quantum ground states with spin-liquid (SL) character. In copper oxides, a SL ground state has recently been experimentally reported on two-dimensional (2D) kagome and triangular lattices [4,5]. In the latter case, numerous competing phases—various SL states, (in)commensurate LRO—have been theoretically predicted for isosceles triangles, depending on the ratio of the two exchange constants [6–8].

Replacing oxygen with other anions is an important step in tailoring physical properties of copper compounds. Transition-metal carbodiimides,  $M(\text{NCN})$ , are good examples for an “organic” route. They are analogs of oxides because the complex anion  $\text{NCN}^{2-}$  is isolobal with  $\text{O}^{2-}$  [9]. Their existence was elusive until very recently, when metathesis reactions lead to the entire family  $M = \text{Mn, Fe, Co, Ni, and Cu}$  [10,11]. The crystal structure of CuNCN (Fig. 1) is orthorhombic ( $Cmcm$ ) and consists of corrugated layers with a 4 + 2 nitrogen environment of  $\text{Cu}^{2+}$  [12,13]. Unlike other  $M(\text{NCN})$  materials, all being AFMs with a Néel temperature around 200–300 K, CuNCN exhibits a nearly temperature ( $T$ ) independent and surprisingly small ( $\chi_b \approx 9 \times 10^{-5}$  emu/mol) bulk magnetic susceptibility, which enhances at low  $T$ , presumably due to a tiny impurity amount [12].

The origin of the surprising reduction in  $\chi_b$  has been debated. Based on local-density approximation calculations, Tsirlin and Rosner predicted a quasi-one-dimensional magnetism, with the leading AFM interaction  $J' \approx 2500$  K bridged via NCN [see Fig. 1(a)] and LRO around 100 K, due to a ferromagnetic interchain interaction  $J_1$  [14]. Neither bulk magnetic nor neutron diffraction (including polarized [13]) measurements, however, could confirm LRO. Liu *et al.* [12] had proposed an alternative model, treating CuNCN as the 2D spatially anisotropic triangular lattice in the  $ab$  plane [Fig. 1(b)]. Their GGA +  $U$  calculations again predicted strong AFM exchange couplings ( $J_1 \approx 800$ – $1000$  K) mediated by N atoms. Their size and the frustrated geometry then lead Tchougréeff and Dronskowski to propose a 2D resonating-valence-bond (RVB) picture with a nonmagnetic SL ground state [15]. These ambiguities about the ground state call for

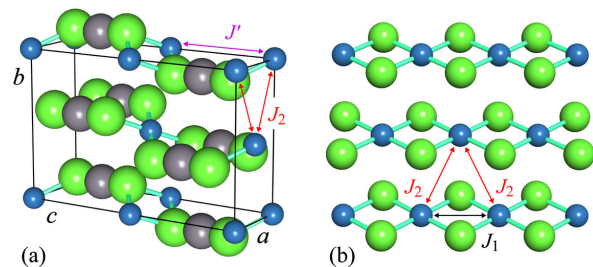


FIG. 1 (color online). (a) Unit cell of CuNCN with blue Cu, green N, and gray C atoms. Exchange couplings are denoted by  $J_1$ ,  $J_2$ , and  $J'$ . (b) Triangular arrangement of Cu atoms in the  $ab$  plane.

detailed *microscopic* investigations, allowing detection of intrinsic *spin-only* susceptibility. In this Letter, we present our local-probe study—including muon-spin relaxation ( $\mu$ SR), nuclear magnetic resonance (NMR), and electron-spin resonance (ESR)—in the temperature range between 63 mK and 300 K. Around 80 K an unconventional magnetically disordered phase develops, implying extreme sensitivity of the magnetic state towards external perturbation. Our results bring forward both similarities and differences between the copper carbodiimide and oxides.

We first turn to  $\mu$ SR, which is an extremely sensitive probe for internal magnetic fields. It can easily distinguish between fluctuating and static magnetism on one hand, as well as between LRO and static disorder on the other [16]. In Fig. 2, we show  $\mu$ SR results in zero magnetic field (ZF) and in a weak transverse field (wTF) of 2 mT, measured on high-purity powder samples [17] at the MUSR facility (ISIS, Rutherford Appleton Laboratory, United Kingdom) and at the General Purpose Surface-Muon Instrument facility (Paul Scherrer Institute, Switzerland). Above 80 K, the ZF muon-spin polarization relaxes according to the relaxation function  $G(t) = G_{\text{VKT}} \cdot \exp[-\lambda t]$  in the Gaussian ( $\beta = 2$ ) limit, with the Voigtian Kubo-Toyabe (VKT) function [18]

$$G_{\text{VKT}}(t) = \frac{1}{3} + \frac{2}{3}[1 - (\Delta t)^\beta] \exp[-(\Delta t)^\beta / \beta]. \quad (1)$$

The dominant relaxation is due to static nuclear-magnetic-fields distribution with the width  $\Delta/\gamma_\mu = 0.16$  mT ( $\gamma_\mu = 2\pi \times 135.5$  MHz/T), while  $\lambda = 0.007 \mu\text{s}^{-1}$  represents a weak dynamical relaxation due to fast fluctuations of electronic magnetic fields.

Below 80 K, the shape of the ZF relaxation function becomes irregular. The amplitude of the high-temperature component decreases at the expense of another, quickly relaxing component [Fig. 2(a)]. The latter prevails below 20 K, where the data again fit well to the VKT

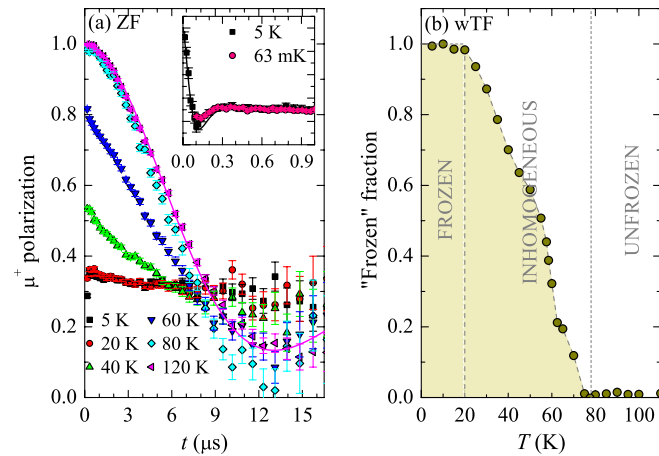


FIG. 2 (color online). (a) Relaxation of muon-spin polarization in zero magnetic field. Solid lines represent fits to Eq. (1); see the text. (b)  $T$  dependence of the frozen fraction, deduced from weak-transverse-field measurements.

relaxation function [Eq. (1)], this time with  $\beta = 1.44$  and significantly increased static internal fields,  $\Delta/\gamma_\mu = 17.7$  mT [inset in Fig. 2(a)]. The largely enhanced  $\Delta$  can be attributed only to electronic fields. The observed dip and the ZF polarization leveling at 1/3 for longer times [19] affirm that local fields are *disordered* and *fully frozen* on the muon time scale [16]. We stress that the absence of coherent oscillation of polarization discards the possibility of a LRO state down to at least 63 mK [inset in Fig. 2(a)].

The wTF measurements further disclose the magnetic state of CuNCN between 80 and 20 K, where multicomponent ZF relaxation is observed. The amplitude of the oscillating polarization, proportional to the fraction of muons still experiencing dynamical electronic fields, gradually decreases in this range. This witnesses progressive development of static internal magnetic fields of electronic origin [“frozen” fraction in Fig. 2(b)], whose magnitudes are large compared to the applied field. This phase is inhomogeneous as part of the muons detect static and the rest dynamical local fields. The wTF measurements confirm a fully static phase below 20 K.

The single-dip ZF muon relaxation observed in CuNCN below 20 K is commonly encountered in spin glasses (SGs) [16]. SG states have been detected by  $\mu$ SR in several frustrated AFMs [20–22] and appear due to some sort of randomness: structural disorder, random fields, bonds or strains, topological defects, etc. One could therefore hastily assign the CuNCN ground state as a SG state. Such state is generally characterized with a pronounced zero-field-cooled–field-cooled (ZFC-FC) irreversibility in  $\chi_b$  below the freezing temperature. We have, therefore, searched for the ZFC-FC irreversibility [17] and for signs of a SG transition in the ac susceptibility in various applied fields between 0.8 mT and 5 T but could not find any. Another peculiarity of CuNCN, uncharacteristic for SGs, is the anomalous stability of the inhomogeneous region of coexisting static (low- $T$ ) and dynamic (high- $T$ ) phases [Fig. 2(b)].

Although low- $T$   $\mu$ SR results in CuNCN reveal static frozen fields, it is the absence of thermal remanence and a well-defined freezing temperature that rules out the canonical SG scenario. A similarly inhomogeneous phase has been reported in the frustrated kagome compound vesignite and reasoned to be due to a vicinity of a quantum critical point [23]. On the other hand, in a few spin-gap systems partially frozen disordered states were unexpectedly detected by  $\mu$ SR [24,25]. They were attributed to a muon locally perturbing exchange pathways, thus prohibiting singlet formation and liberating spin degrees of freedom in its vicinity [26,27]. For slow dynamics, a local-probe muon would not distinguish such a state from collective spin freezing. This is plausible in CuNCN, as muons are likely to stop near bridging N atoms of the  $\text{NCN}^{2-}$  groups, similarly as protons are positioned in related  $M(\text{NCNH})_2$  ( $M = \text{Fe-Ni}$ ) [28].

To avoid any disturbance of the CuNCN structure by external probes, we next decided to employ  $^{14}\text{N}$  ( $I = 1$ )

NMR measurements because intrinsic  $^{14}\text{N}$  nuclei also directly detect local magnetic fields. To obtain a reasonable signal-to-noise ratio, the frequency-swept spectra were measured in a high magnetic field of 9.4 T [29].

At 250 K, the NMR spectrum (Fig. 3) exhibits a characteristic quadrupolar powder line shape, which allows fixing the quadrupolar interaction parameters  $\nu_Q = 0.79(2)$  MHz and  $\eta_Q = 0.06(2)$ . In order to simulate the low- $T$  spectra, we assume a convolution with a  $T$ -dependent Gaussian local-field distribution with the width  $\sigma(T)$  originating from the hyperfine coupling between the nuclear and  $\text{Cu}^{2+}$  electronic moments.  $\sigma$  starts increasing below 200 K and more dramatically below ca. 100 K [Fig. 3(a)]. However, it fails to scale with the moderate increase of  $\chi_b$  at low  $T$  [Fig. 3(a)], thus ruling out the distribution of hyperfine couplings as the source of the spectral broadening. Moreover, spin-spin relaxation measurements (not shown) discard an increase in the relaxation rate as a possible origin of the low- $T$  broadening, which is therefore inhomogeneous and due to a broad distribution of local susceptibilities (*static electronic moments*) at low  $T$  and high fields.

The  $T$  dependence of the  $^{14}\text{N}$  spin-lattice relaxation rate  $1/T_1$ , measured with an inversion recovery technique, reveals the development of electronic spin dynamics since the fast spin-lattice relaxation times of only a few milliseconds [Fig. 3(b)] directly measure the local-field fluctuations [Fig. 3(b)] directly measure the local-field fluctuations weight at the Larmor frequency. The  $^{14}\text{N}$  magnetization relaxation curves were analyzed with the stretched exponential model  $M_z(t) - M_0 \propto \exp[-(t/T_1)^\alpha]$ . Although  $1/T_1$  shows no obvious anomaly at 80 K, the stretch exponent  $\alpha$  clearly starts to decrease below 80 K and reaches a value of 0.5 at lowest  $T$  [inset (i) in Fig. 3(b)]. This evidences that the distribution of relaxation rates widens below 80 K—another hallmark of a magnetically highly disordered state. Around 20 K, a  $1/T_1$  maximum is observed [inset (ii) in Fig. 3(b)], indicating freezing of spin

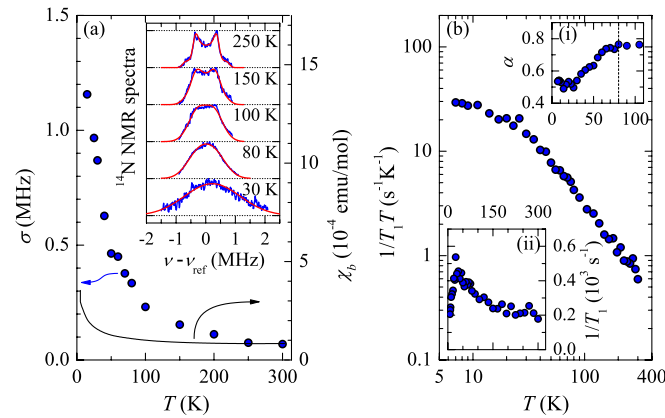


FIG. 3 (color online). (a) Comparison of Gaussian broadening  $\sigma$  of  $^{14}\text{N}$  NMR spectra and bulk susceptibility  $\chi_b$  (in 5 T). Inset: Simulation (red lines) of selected experimental (blue lines) spectra. (b) Spin-lattice relaxation rate  $1/T_1$  divided by  $T$ . Inset:  $T$  dependence of (i) the stretch exponent and (ii)  $1/T_1$ .

dynamics below this temperature. The freezing is moderate, far from opening of a spin gap, which would require a suppression of  $1/T_1 T$ , not observed experimentally [Fig. 3(b)]. A ZF spin gap could however be closed by the large applied field of 9.4 T [8].

The electronic properties of CuNCN were, therefore, also investigated at much lower fields ( $B_0 \approx 0.33$  T) with continuous-wave ESR measurements in the X band ( $\nu_L = 9.6$  GHz), following both FC and ZFC temperature treatments. The ESR spectra [inset (i) in Fig. 4(a)] comprise two overlapping components: a broad Lorentzian component with the RT linewidth of 280(10) mT and a ca. 10-times narrower Gaussian component. The RT  $g$ -factor value  $g = 2.07$  of the broad component is common for  $\text{Cu}^{2+}$  in a square planar environment [30]. The broad-component ESR intensity, corresponding to the spin-only susceptibility, was calibrated at RT with a couple of standards:  $\chi_{\text{ESR}}^{\text{RT}} \approx 9(1) \times 10^{-5}$  emu/mol. It is the same as the bulk susceptibility, which proves that the broad component represents the intrinsic ESR signal. The narrow component, on the other hand, is ca. 100 times less intense and exhibits a Curie-like  $T$  dependence. The total fraction of impurity spins contributing to it is estimated as only 0.04%. The intrinsic ESR component exhibits a minimum in the linewidth and a maximum in the  $g$  factor around 130 K [Fig. 4(b)]. Both indicate growth of spin correlations [30], which appear particularly strong below  $\sim 80$  K. The featureless  $T$  dependence of both parameters and no obvious ZFC-FC dissimilarities of ESR spectra speak against a conventional SG transition, in line with the lack of usual susceptibility fingerprints of such a state. Moreover, the intrinsic  $\chi_{\text{ESR}}$  rapidly diminishes below 80 K, thus diverging from  $\chi_b$  [Fig. 4(a)].

The suppressed  $\chi_{\text{ESR}}$  implies opening of a spin gap and thus allows for an alternative interpretation of the magnetic state in CuNCN. For the anisotropic triangular lattice, Hayashi and Ogata proposed that in ZF two spin-singlet

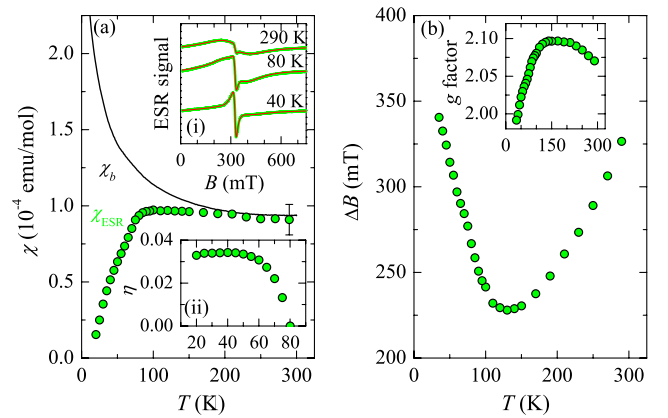


FIG. 4 (color online). (a) Comparison of bulk susceptibility  $\chi_b$  and ESR spin-only susceptibility  $\chi_{\text{ESR}}$ , both measured in 0.33 T. Inset: (i) Fits (red lines) of selected ESR spectra (green lines) and (ii)  $T$  dependence of the 2D RVB order parameter. (b)  $T$  dependence of the ESR linewidth and the  $g$  factor (inset).

states are formed at different temperatures, depending on the  $J_2/J_1$  ratio [31]. Below the upper critical temperature  $\theta_c = 3J_1/8$ , a quasi-1D gapless RVB phase sets in, while a 2D gapped RVB phase appears at the lower critical temperature  $\theta'_c = J_2/8(1 - 2J_2/3J_1)$  [15]. We have further developed the analytical susceptibility expression [15] for the 2D RVB phase and arrive at

$$\chi = \mu_B^2 \left\{ \frac{(1 - ca)f(3\sqrt{2}J_2\eta)}{3\sqrt{2}(J_1\xi - J_2\eta)} - ca \frac{\partial f}{\partial \varepsilon}(3\sqrt{2}J_2\eta) \right\}, \quad (2)$$

where  $a = J_2\eta/J_1\xi$ , with  $\xi$  and  $\eta$  as the 1D and 2D RVB order parameters, respectively;  $f$  is a Fermi distribution function, and  $c = 1 + (1 - \frac{3B}{4} + \frac{1}{2}B \ln a) \frac{a}{1-a}$  [32]. Assuming constant  $\xi = 1/\sqrt{2}\pi$  [15] in the 2D RVB phase, we estimate the exchange constants  $J_1 = 2300$  K and  $J_2 = 540$  K and establish the  $T$  dependence of the 2D RVB order parameter [inset (ii) in Fig. 4(a)] from  $\chi_{\text{ESR}}(T)$  for  $\theta'_c = 80$  K.

We note that both RVB phases are characterized by complete spin pairing, in agreement with no magnetic neutron scattering in polarized experiments [13]. The growing spin correlations observed in ESR are also in line with the 2D RVB phase below  $\theta'_c$ . This phase, however, appears to be very fragile, as muons can locally distort singlets and lead to static local states within the spin gap  $\Delta_s$  below  $\theta'_c$ . Moreover, as  $\Delta_s = 3\sqrt{2}J_2\eta$  is comparable to the applied magnetic field in NMR, it is reasonable to assume that the lack of the spin gap and the growing static fields observed in NMR may be field-induced. This calls to mind the recently discovered emergence of inhomogeneous moments in extremely weak fields on another triangular lattice [33] and points to the importance of frustration, which amplifies the role of small perturbations in selecting between competing spin-liquid and more conventional frozen phases.

In conclusion, CuNCN, the first nitrogen-based analog of CuO, with a surprisingly low magnetic susceptibility, lacks magnetic ordering down to at least 63 mK. A magnetically highly disordered state has been witnessed below 80 K by complementary local probes. Alternatively to a SG-like frozen state featuring an unprecedented broadness of inhomogeneous static and dynamic phase, no well-defined freezing temperature, and no conventional susceptibility-fingerprint SG features, a dynamical spin liquid is proposed. The fragility of the electronic state to perturbations seems to be a peculiarity of carbodiimides as opposed to more conventional oxides.

P. Müller, V. Feldman, F. Haarmann, P. Mendels, and F. Bert are gratefully acknowledged for valuable discussion. We thank H. Luetkens and A.D. Hillier for technical assistance with  $\mu$ SR. We acknowledge the financial support of the Slovenian Research Agency (Project No. J1-2118), the Russian Foundation for Basic Research (Grant No. 10-03-00155), and the German Science Foundation. The  $\mu$ SR measurements were supported by the European Commission (Contract No. CP-CSA\_INFRA-2008-1.1.1 226507-NMI3).

- [1] P. A. Lee *et al.*, *Rev. Mod. Phys.* **78**, 17 (2006).
- [2] L. Balents, *Nature (London)* **464**, 199 (2010).
- [3] *Introduction to Frustrated Magnetism*, edited by C. Lacroix, P. Mendels, and F. Mila (Springer-Verlag, Berlin, 2011).
- [4] P. Mendels *et al.*, *Phys. Rev. Lett.* **98**, 077204 (2007).
- [5] H. D. Zhou *et al.*, *Phys. Rev. Lett.* **106**, 147204 (2011).
- [6] Z. Weihong, R. H. McKenzie, and R. P. Singh, *Phys. Rev. B* **59**, 14367 (1999).
- [7] S. Yunoki and S. Sorella, *Phys. Rev. B* **74**, 014408 (2006).
- [8] O. A. Starykh, H. Katsura, and L. Balents, *Phys. Rev. B* **82**, 014421 (2010).
- [9] M. Launay and R. Dronskowski, *Z. Naturforsch. B* **60**, 437 (2005).
- [10] X. Liu *et al.*, *Inorg. Chem.* **44**, 3001 (2005); X. Liu *et al.*, *Z. Naturforsch. B* **60**, 593 (2005).
- [11] M. Krott *et al.*, *Inorg. Chem.* **46**, 2204 (2007); X. Liu *et al.*, *Chem. Eur. J.* **15**, 1558 (2009).
- [12] X. Liu *et al.*, *J. Phys. Chem. C* **112**, 11013 (2008).
- [13] H. Xiang *et al.*, *J. Phys. Chem. C* **113**, 18891 (2009).
- [14] A. A. Tsirlin and H. Rosner, *Phys. Rev. B* **81**, 024424 (2010).
- [15] A. L. Tchougréeff and R. Dronskowski, [arXiv:1008.0182](https://arxiv.org/abs/1008.0182).
- [16] *Muon Science: Muons in Physics, Chemistry, and Materials*, edited by S. L. Lee, S. H. Kilcoyne, and R. Cywinski (Taylor & Francis, Abingdon, 1999).
- [17] See Supplemental Material at <http://link.aps.org/supplemental/10.1103/PhysRevLett.107.047208> for details on sample preparation, characterization, and bulk magnetization measurement.
- [18] M. R. Crook and R. Cywinski, *J. Phys. Condens. Matter* **9**, 1149 (1997).
- [19] In powders, polarization of 1/3 of all muons does not relax because it is parallel to the internal field.
- [20] S. R. Dunsiger *et al.*, *Phys. Rev. B* **54**, 9019 (1996).
- [21] A. Harrison *et al.*, *Physica (Amsterdam)* **289B**, 217 (2000).
- [22] C. R. Wiebe *et al.*, *Phys. Rev. B* **68**, 134410 (2003).
- [23] R. H. Colman *et al.*, *Phys. Rev. B* **83**, 180416 (2011).
- [24] D. Andreica *et al.*, *Physica (Amsterdam)* **289B**, 176 (2000).
- [25] Y. Fudamoto *et al.*, *Phys. Rev. B* **65**, 174428 (2002).
- [26] J. A. Chakhalian *et al.*, *Phys. Rev. Lett.* **91**, 027202 (2003).
- [27] A. A. Aczel *et al.*, *Phys. Rev. B* **76**, 214427 (2007).
- [28] M. Krott *et al.*, *J. Solid State Chem.* **180**, 307 (2007); X. Tang *et al.*, *Z. Anorg. Allg. Chem.* **637**, 1089 (2011).
- [29] We used pulse sequence  $\beta$ - $\tau$ - $\beta$ - $\tau$ -echo, pulse length  $\tau_\beta = 8 \mu\text{s}$ , interpulse delay  $\tau = 60 \mu\text{s}$ , and repetition time 100 ms at RT. The  $^{14}\text{N}$  reference frequency of 28.9027 MHz was determined from the  $\text{CH}_3\text{NO}_2$  standard.
- [30] A. Abragam and B. Bleaney, *Electron Paramagnetic Resonance of Transition Ions* (Clarendon, Oxford, 1970).
- [31] Y. Hayashi and M. Ogata, *J. Phys. Soc. Jpn.* **76**, 053705 (2007); *J. Phys. Conf. Ser.* **150**, 042053 (2009).
- [32] With  $B = 3.72$ , this allows us to reproduce the numerically established mean-field 2D RVB gap dependence on the anisotropy  $\sim \exp(-bJ_1/J_2)$ , with  $b = 1.61$  [31].
- [33] F. L. Pratt *et al.*, *Nature (London)* **471**, 612 (2011).